CrossMark

ORIGINAL PAPER

Facile one-step extraction and oxidative carboxylation of cellulose nanocrystals through hydrothermal reaction by using mixed inorganic acids

Miao Cheng · Zongyi Qin · Yuanyu Chen · Jiaming Liu · Zichu Ren

Abstract A facile and efficient approach to prepare carboxylated cellulose nanocrystals (CCNCs) is presented through a novel one-step hydrothermal procedure by using a mixed acid system of hydrochloric acid and nitric acid (HCl/HNO$_3$). The as-prepared cellulose nanoparticles were characterized by scanning electron microscopy, wide angle X-ray diffraction, conductometric titrations, Fourier transform infrared spectrometry and thermal gravimetric analysis. The results showed that the combination of the mixed acid and hydrothermal reaction can speed up the process of CCNC preparation, and then high quality of the product could be obtained at relatively low acid concentration. It is found that the addition of nitric acid could not only promote the conversion of surface groups on the cellulose nanocrystals (CNCs), but also have significant influences on the yield, particle size and microstructure of CNCs. For the volume ratio of HCl/HNO$_3$ of 7:3, the as-prepared CCNCs exhibited the largest length to diameter ratio and narrowest dimension distributions as well as maximum degree of oxidation of 0.12. In addition, high dispersion stability for the CCNCs could be observed due to the existence of negative carboxyl groups. This approach based on one-step oxidative carboxylation greatly simplified the preparation of CCNCs with high yield and high crystallinity under mild hydrothermal condition.

Keywords Carboxylated cellulose nanocrystals · Mixed acid hydrolysis · Hydrothermal reaction · One-step oxidative carboxylation

Introduction

Cellulose nanocrystals (CNCs) have successfully been used for a wide spectrum of applications spanning from nanocomposites, packaging, and mechanical and rheological property modifications, to chemical catalysis and organic templating, benefiting from their numerous advantages such as renewability, sustainability, biocompatibility, and cost efficiency (Moon et al. 2011; Yu et al. 2013a, b; Jonoobi et al. 2015). As organic reinforcements, the CNCs possess intriguing mechanical properties such as transverse elastic modulus of 18–50 GPa and anisotropic elastic modulus of 140–220 GPa, large length to diameter ratio, and low density of about 1.6 g cm^{-3}. The increasing mechanical strength has been explained by specific interactions such as strong hydrogen bonding between the CNCs and polymeric matrix. However, the CNCs were generally produced by the acid hydrolysis of cellulose-rich sources, and the CNCs have numerous

M. Cheng · Z. Qin (✉) · Y. Chen · J. Liu · Z. Ren
State Key Laboratory for Modification of Chemical Fibers and Polymer Materials, and College of Material Science and Engineering, Donghua University, Shanghai 201620, China
e-mail: phqin@dhu.edu.cn

Springer

surface hydroxyl groups, which inherently exhibit low dispersibility in polymer matrix and poor interfacial interactions, particularly as nanofillers with hydrophobic matrix polymers (Chen et al. 2016a, b; Leung et al. 2011). Fortunately, depending on the desired application, chemical modification of the CNCs can be carried out at the hydroxyl groups of the glucose units on the crystalline backbone structure (Lam et al. 2012a). The introduction of carboxyl groups to CNCs can enhance the interfacial interaction with hydrophobic polymeric matrix by improving their dispersion stability in various organic solvents which are good solvents for the polymer, take part in covalent crosslinking and grafting reactions, drive the adsorption of small molecules and ions, as well as make them highly efficient as templates for anchoring functional inorganic nanoparticles (Leung et al. 2011; Eyley and Thielemans 2014; Yu et al. 2013a, b; Moon et al. 2011; Fujisawa et al. 2013; Hosseinidoust et al. 2015). It has been shown that carboxyl groups can be introduced on the surface of CNCs, resulting in a higher surface charge compared with sulfuric acid hydrolyzed CNCs, through either a pre-or post-treatment by using 2,2,6,6,-tetramethylpiperidine-1-oxyl (TEMPO) mediated oxidation in addition to acid hydrolysis (Zhang et al. 2016; Qin et al. 2011; Montanari et al. 2005). However, the control of such oxidation process was so complicated. For example, the pH of the reaction system should be kept at 10 for 5 h. Recently, carboxylated CNCs (CCNCs) with yields of 14–81% were successfully extracted from various cellulosic sources through one-step hydrolysis of ammonium persulfate (APS), a strong oxidant, instead of acid hydrolysis (Zhang et al. 2016; Cheng et al. 2014; Castro-Guerrero and Gray 2014; Mascheroni et al. 2016; Leung et al. 2011). It is suggested that TEMPO is only effective in fiber defibrillation, that is to say, it does not completely break down the amorphous domains (Leung et al. 2011). Therefore cellulose starting materials are often hydrolyzed under acid conditions firstly and then are oxidized further by the TEMPO-mediated oxidation for yielding CCNCs. For ultrasonic assisted TEMPO-mediated oxidation, CCNCs having high carboxylate content were produced directly (Qin et al. 2011). It has higher yield of CCNCs but larger energy consumption and quite expensive compared with one-pot APS oxidation. However, the amount of APS used in the reaction is large, the yield of CCNCs is lower, and the reaction temperature is high, although APS defibrillated and removed amorphous cellulose effectively. Note that two-step oxidation has been also reported to prepare CNCs with sodium periodate followed by sodium chlorite (Yang et al. 2013; Sirviö et al. 2015).

For the production of CNCs, the classic and most widely used method is acid hydrolysis of a purified cellulose starting material. Different inorganic acids including sulfuric, hydrochloric, nitric, tungstophosphoric, hydrobromic and phosphoric acids or their mixtures have been used as reaction medium for the extraction of CNCs (Yu et al. 2013a, b; Camarero Espinosa et al. 2013; Xiong et al. 2012; Hamid et al. 2016; Jonoobi et al. 2015). Moreover, some organic acids such as oxalic acid, maleic acid, p-toluenesulfonic, and benzenesulphonic acids were also used to prepare CNCs recently (Chen et al. 2016a, b; Sirviö et al. 2016). Sulfuric acid and hydrochloric acid were widely used to produce the CNCs from various cellulose-rich sources. These CNCs are usually elongated rods with high length to diameter ratio depending on the source of cellulose and hydrolysis conditions. The CNCs prepared by sulfuric acid hydrolysis have negatively charged surfaces due to the esterification of hydroxyl groups incorporated by sulfate ions, whereas no known surface modification occurred for hydrochloric acid hydrolysis, and only few charges could be found on the surface of the CNCs (Yu et al. 2013a, b). In general, the CCNCs were obtained through a route to first hydrolyze cellulose raw materials, then chemically modify with oxide acids or oxidation (Yu et al. 2013a, b; Yu et al. 2016). For example, Tong et al. dispersed firstly cotton into 64% sulfuric acid and treated at 45 °C for 45 min, then dialyzed with distilled water for 7 days, and finally reacted with succinic anhydride at 120 °C for 12 h (Yu et al. 2013a, b). Recently, some mixed reaction systems such as HNO_3/H_3PO_4–$NaNO_2$ were used to prepare carboxyl functionalized cellulosic nanoparticles (Kumar and Yang 2002; Xu et al. 2014; Sharma and Varma 2014).

Generally, alteration of the surface chemistry is performed by using multiple reaction steps. Although some single-step methods for the extraction and surface functionalization of CNCs have successfully used for various cellulose-based raw materials by using APS and the acid mixture composed of hydrochloric and an organic acid such as formic and citric acid, but requiring too long reaction time for

industrial use (Zhang et al. 2016; Cheng et al. 2014; Castro-Guerrero and Gray 2014; Mascheroni et al. 2016; Leung et al. 2011; Chen et al. 2016a, b; Sun et al. 2016a; Yu et al. 2016). It may be argued that this slow hydrolysis rate might result mainly from the configuration itself of cellulose. It is known that hydrothermal treatment could enhance the possibility of acid attack (Yu et al. 2013a, b). In this work, a high-efficiency one-step approach through a mixed acid system of hydrochloric acid and nitric acid (HCl/HNO₃) hydrolysis of microcrystal celluloses (MCCs) under hydrothermal condition was reported for the extraction of CCNCs. The using of HNO_3 as an oxidant can be expected to effectively modify the hydroxyl groups on the surface of CNCs with carboxyl groups. More attention is paid to optimize nitric acid fraction to obtain a high yield and good stability of CNC aqueous suspensions.

Experimental

Materials

Commercial MCCs ($M_w = 36,000$) as starting materials for extracting CCNCs were purchased from Shanghai Chemical Reagents (Shanghai, China). Hydrochloric acid (HCl) and nitric acid (HNO_3) were purchased from Guoyao Group Chemical Reagent CO., LTD. All the material and reagents were used as received without further purification.

Preparation

The CCNCs were extracted from the MCCs according to a modified hydrothermal method with a mixed acidic medium of HCl/HNO₃ instead of pure HCl (Yu et al. 2013a, b). Briefly, 1 g MCC was hydrolyzed in the hydrothermal kettle at 110 °C for 3 h by using 60 mL HCl/HNO₃ mixed acid with various volume ratios including 9:1, 8:2, 7:3, 6:4, and 5:5, respectively. Considering the addition of HNO_3 as the strong oxidizing acid, the concentration of mixed acid used in this work was reduced to 4 M instead of 6 M pure HCl used in previously reported. After cooling to room temperature, the resultant suspension was diluted, and then repeatedly washed by successive centrifugations with deionized water to ensure the removal of free acids. The as-prepared product was redispersed under sonication (Kunshan Ultrasonic Instruments Co., Ltd, China; 50 W, 40 Hz) for 5 min for forming a stable aqueous suspension. Besides a small amount of suspension was used to characterize the stability of suspension and measure the particle size distribution and zeta potential, most of them were finally freeze-dried for 48 h to obtain the CCNCs. For comparison, the CNCs were prepared in 4 M pure HCl medium under the same preparation process.

Characterization

The morphologies of as-prepared CNCs were observed on a field emission scanning electron microscopy (FE-SEM, HITACHI S-4800) at 1.0 kV. The CNCs were deposited on silicon dices and the sizes of nanorods were measured from FE-SEM images.

The particle size distribution and zeta potentials for the CNC suspensions were measured on a Nano ZS Malvern Zetasizer equipment with both multi-angle particle size analysis by dynamic light scattering and low-angle zeta potential analysis by electrophoretic light scattering. The measurements for 2.5 mg/mL CNC suspensions were conducted in triplicate for each sample, and each sample was scanned 5 times and results were averaged for each measurement.

The chemical structures were characterized on a Nicolet 8700 Fourier transform infrared spectrometer (FT-IR). The samples were analyzed as KBr pellets (1% cellulose in anhydrous KBr). FT-IR spectra were recorded in the spectral range of 4000–400 cm⁻¹ with a resolution of 4 cm⁻¹ and an accumulation of 64 scans. The degree of oxidation (DO) measurements were achieved by calculating the ratio of the intensity of the absorption band near 1730 cm⁻¹, corresponding to the carbonyl stretching frequency, to that of the strongest band near 1050 cm⁻¹, intrinsic of the cellulose backbone.

The crystal structures were characterized on a Philips PZ1200 X-ray diffractometer by using Cu Kα(1.5418 Å) X-rays with a voltage of 40 kV and a current of 30 mA. X-ray diffraction data were collected over an angular range of 5–40° at the rate of 2°/min in steps of 0.02° at room temperature. The crystallinity index (CrI) of the samples was determined by Segal's equation:

$$CrI = \left[\left(I_{(200)} - I_{(am)} \right) / I_{(200)} \right] \times 100\% \qquad (1)$$

where $I_{(200)}$ is the intensity of the crystalline peak at the maximum at 2θ between 22° and 23°, $I_{(am)}$ the intensity at the minimum at 2θ between 18° and 19°, and θ is the corresponding Bragg angle.

The carboxyl content of oxidized cellulose samples was determined by conductimetric titration, being based on the fact that during the titration, one of the ions is replaced by the other and invariably these two ions differ in the ionic conductivity with the result that conductivity of the solution varies during the course of titration (Araki et al. 1998; Mascheroni et al. 2016). The cellulose samples (25 mg) were suspended into 15 mL of 0.01 M hydrochloric acid solutions. After 10 min of stirring, the suspensions were titrated with 0.01 M NaOH. The conductimetric titration curve for the suspension first showed a decrease in conductivity corresponding to the neutralization of strong acid in solution. The horizontal portion after the first inflection point corresponds to the neutralization of weak acid groups (probably carboxylic acid) on CNCs. After the equivalence point is achieved the conductivity increases rapidly due to the excess NaOH. The DO value was given by the following equation:

$$DO = 162C(V_2 − V_1)/[C(w − 36)(V_2 − V_1)] \quad (2)$$

where V_1 and V_2 are the volume of NaOH (L) corresponding to first inflection point and the equivalence point at conductimetric titration curve, respectively, $(V_2−V_1)$ is the volume of NaOH (L) required to deprotonate the carboxylic acids groups, C the NaOH concentration (mol/L), and w the weight of the dried sample. The value of 162 corresponds to the molar mass of anhydrous glucose unit (AGU), and the value of 36 to the difference between the molecular weight of an AGU and that of the sodium salt of a glucuronic acid moiety. The change in conductivity was recorded by a conductometer (DDSJ-308F).

The thermal stability was studied on a NETZSCH TG 209 F1 thermogravimetric analyzer. 0.3 mg CNC (or CCNC) powder was directly placed in a ceramic crucible for TGA measurement. The measurements were performed from room temperature to 600 °C at a heating rate of 20 °C/min in a nitrogen atmosphere with a flow rate of 20 mL/min. The degradation parameters including initial decomposition temperature (T_0), the 5% weight loss temperatures ($T_{5\%}$) and maximum decomposition temperature (T_{max}) were calculated from the TGA curve.

Results and discussion

Morphology and suspension stability

Oxidized cellulose containing carboxyl groups is commercially available by reacting cellulose with NO_2 or N_2O_4 in the gaseous form or as a solution in an appropriate organic solvent, and the reaction with HNO_3 alone requires heating at high temperature, these cause extensive hydrolysis of cellulose and low yield of oxycellulose (Xu et al. 2014). Generally, the extraction of CNCs from cellulose-rich raw materials can be achieved through inorganic acid hydrolysis, in which the disordered or paracrystalline regions of cellulose could be hydrolyzed whereas crystalline regions exhibited a higher resistance to acid attack (Domingues et al. 2014; Sun et al. 2016b; Jiang et al. 2010). The yields and size distribution of the CNCs depended strongly on acid concentration, reaction temperature, and reaction time. It is demonstrated that hydrothermal systems can provide a special reaction under high pressure and high temperature condition, resulting in facile and rapid extraction of thermally stable CNCs from commercial MCCs with a yield up to 93% in 6 M hydrochloric acid solution at 110 °C for 3 h (Yu et al. 2013a, b). To satisfy the requirement of new properties of cellulose, carboxyl groups would be introduced onto a polymer surface through the oxidization of secondary hydroxyl groups of the pyranose ring in cellulose. Herein nitric acid as a strong oxidizing agent was mixed with hydrochloric acid solution in a hydrothermal reaction kettle. Keeping reaction time of 3 h and temperature of 110 °C, the acid concentration was reduced from 6 M to 4 M to avoid excessive degradation of cellulose. The morphologies of as-prepared CNCs were displayed in Fig. 1. It is found that all the CNCs possessed a rod-like structure, but the products prepared in mixed acid medium exhibited more well-dispersion and smaller dimension compared with that in pure hydrochloric acid solution as listed in Table 1. The morphologies of the CNCs and CCNCs were further observed by TEM as displayed in Fig. 2. Compared with that extracted by using pure HCl medium, the average length of CNCs decreased from 256 ± 30 to 213 ± 27, 196 ± 33, 165 ± 31, 170 ± 36 and 185 ± 23 nm with the increase content of HNO_3, meanwhile the average width also reduced from 23 ± 5 to 21 ± 3, 20 ± 9, 13 ± 3 13 ± 5 and
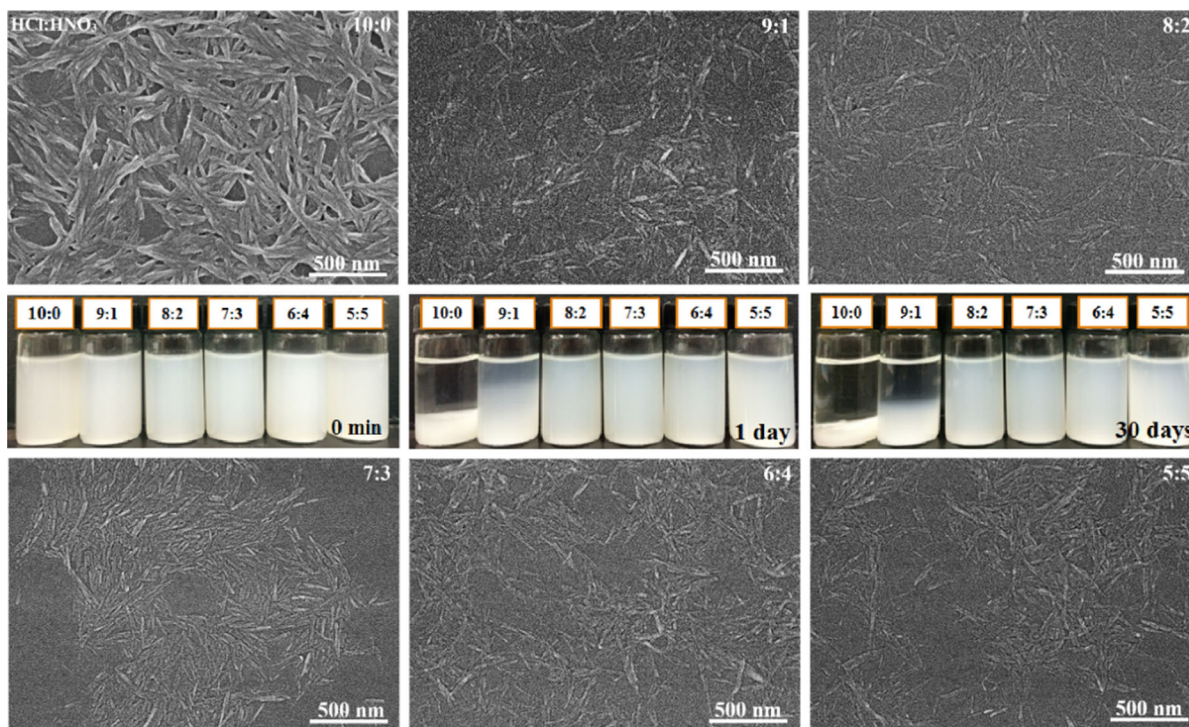
Fig. 1 FE-SEM images and suspension stability of the CNCs and CCNCs prepared under various acidic conditions

Table 1 Dimension, Zeta potential and yield for the CNCs prepared under various acidic conditions

Sample	HCl:HNO$_3$ (v/v)	Length (nm)[a]	Diameter (nm)[a]	Size (nm)[b]	Zeta potential (mV)	Yield (%)
CNCs	10:0	245 ± 25	24 ± 11	386	−6.7	84.6
CCNCs	9:1	199 ± 19	18 ± 5	230	−18.4	82.5
	8:2	193 ± 14	17 ± 4	212	−34.5	75.2
	7:3	176 ± 6	11 ± 2	188	−45.3	72.6
	6:4	184 ± 16	14 ± 2	206	−39.1	73.9
	5:5	187 ± 18	14 ± 4	218	−33.3	76.8

[a] Length and diameter were measured from SEM images

[b] Size was calculated by DLS particle size analyzer

14 ± 6 nm, respectively. Due to the decrease in acid concentration, the average length and width of the CNCs became larger but still close to that extracted by using 6 M hydrochloric acid reported in the previous work. Furthermore, reduction in dimension of the CNCs in mixed acid medium illustrated the acceleration of hydrolysis process in the presence of nitric acid. More clearly, the dimension and yield decreased first with the increase of nitric acid fraction, reached a minimum value at the volume ratio of HCl and HNO$_3$ of 7:3, and then increased. The minimum length and width for the CNCs were 176 ± 6 and 11 ± 2 nm, respectively, while the yield decreased from 84.6 for single acid hydrolysis to 72.6%, which was still larger than those reported by most previous works involving inorganic acid hydrolysis (Zhang et al. 2016; Mascheroni et al. 2016).

Figure 1 also gives the suspension stability of the CNCs and CCNCs prepared under various acidic conditions. After ultrasonication, all the CNC
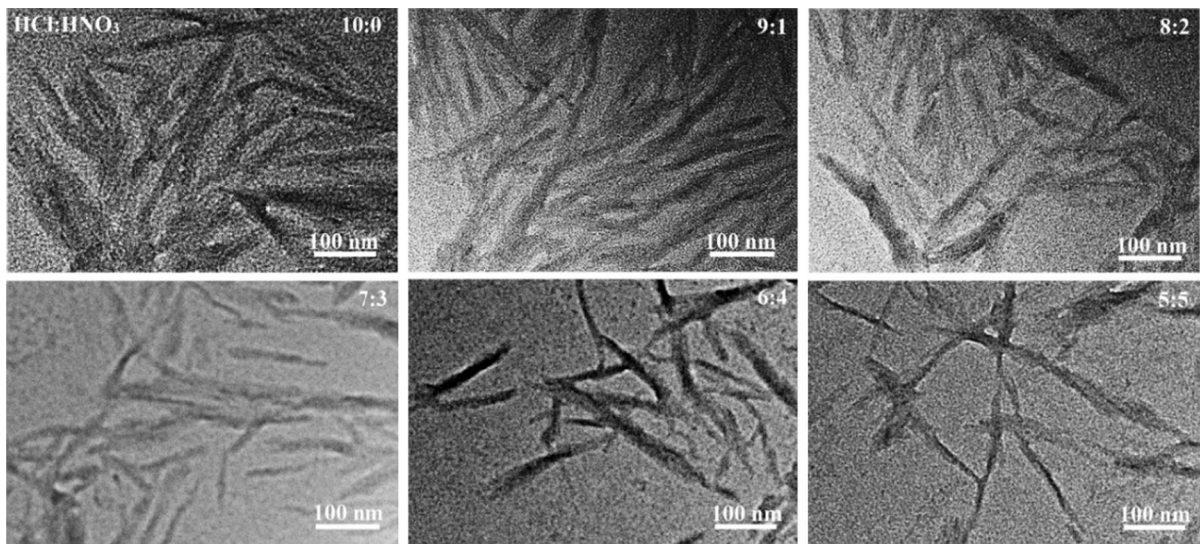
Fig. 2 TEM images of the CNCs and CCNCs prepared under various acidic conditions

suspensions were blue in color and no obvious sedimentation can be observed at the bottom of the bottle. As the time prolonged, lots of sedimentations appeared and after 1 day, almost all the CNCs prepared without nitric acid would deposit onto the bottom of glass bottle. The CNCs prepared by pure HCl hydrolysis were easy to aggregate together due to the strong hydrogen bonding between the nanoparticles having numerous surface hydroxyl groups as shown in Fig. 1. By contrast, excellent suspension stability could be observed for the CNCs extracted in mixed acid medium, and after 30 days, these suspensions still kept high stability. It is believed that the existence of carboxyl groups on the surface the CNCs in the presence of nitric acid could provide strong electrostatic repulsions to avoid the particle aggregation, which could significantly enhance their reinforcing effects in hydrophilic polymeric matrix (Yu et al. 2016; Xiong et al. 2012).

Size distribution and Zeta potential

Dynamic light scattering (DLS) and Zeta potential measurements have gained popularity as simple, easy and reproducible tools to ascertain particle size and surface charge. The average size obtained from DLS data is a hypothetical measurement as such hard spheres rarely exist in colloidal dispersions (Yu et al. 2013a, b; Cheng et al. 2014; Hosseinidoust et al. 2015). Thus for rod-like CNCs, the measurements

were only used to compare relative particle sizes. As represent in Table 1, the average size of the CNCs decreased from 386 nm for pure hydrochloric acid to 230 nm when 10% (V/V) nitric acid was added into the reactive medium. With the increase of nitric acid fraction, the average size further decreased to the minimum value of 188 nm for the volume ratio of HCl and HNO_3 of 7:3, and then increased to 218 nm for equal volume of HCl and HNO_3. The trend of variation is in agreement with that of SEM experiments.

One of the most popular uses of zeta potential data is to relate it with suspension stability, and the electrostatic repulsion is believed to be the physical mechanism for stabilizing most aqueous nanoscale particle systems. At this point, it is considerable that the nanoparticle dispersions can be classified as highly unstable, relatively stable, moderately stable and highly stable according to zeta potential values of ± 0–10 mV, ± 10–20 mV and ± 20–30 mV and $> \pm 30$ mV, respectively (Bhattacharjee 2016). The yield and Zeta potential of CNCs prepared under various acidic conditions as shown in Fig. 3 and Table 1 lists Zeta potential value for the CNCs prepared under various acidic conditions, and all of the CNC suspensions had negative zeta potential values. Due to the lack of negative surface charges, the CNCs extracted through pure hydrochloric acid hydrolysis would rapidly aggregate. The increase in the absolute value of zeta-potential is resulted from the conversion from surface hydroxyl groups to carboxyl groups when the nitric acid as the strong oxidation agent was
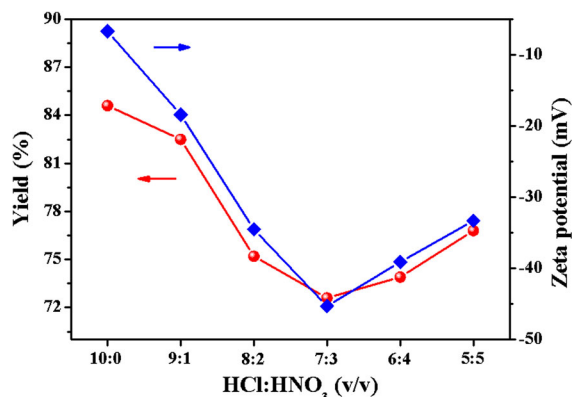
Fig. 3 Yield and Zeta potential of CNCs and CCNCs prepared under various acidic conditions

introduced into the reaction system (Cheng et al. 2014; Mascheroni et al. 2016)). Larger the absolute value of zeta potential, better suspension stability that can be achieved due to electrostatic repulsion between the nanoscale particles, which is consistent with the observations of the stability of the suspensions. Moreover, the zeta potential value of CNCs was first decreased and then increased with the increase of nitric acid fraction. A minimum value of -45.3 appeared at the ratio of HCl and HNO_3 of 7:3, implying under this condition, the strongest oxidation effect occurred.

Chemical structure

Figure 4 shows the FT-IR spectra of the CNCs extracted under various acidic conditions. It is found that all the CNCs exhibited typical absorption bands of cellulose. The very broad band around 3400 cm^{-1} is
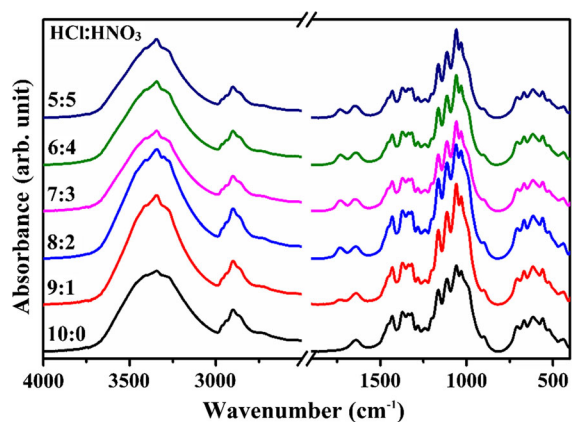

Fig. 4 FT-IR spectra of CNCs and CCNCs prepared under various acidic conditions

assigned to the stretching vibrations of –OH groups, with a contribution near 2900 cm^{-1} due to the stretching vibrations of C–H bonds. There are three different hydroxyl groups present, located at C2, C3, and C6 positions, contributing to the formation of different kinds of intra-and intermolecular hydrogen bonds. The hydrogen bonding of cellulose would be weakened for the CNCs extracted through acid hydrolysis, resulting in that the –OH stretching vibration bands became narrow and shifted towards lower wavelength. The characteristic bands at 1160 and 897 cm^{-1} were corresponded to C–O–C bending and symmetric stretching at the ß − (1 → 4) -glycosidic linkage, and at 1060 and 1113 cm^{-1} to C–O–C stretching of pyranose and glucose ring skeletal vibration, respectively. These characteristic peaks indicated that all the samples are primarily in the form of cellulose I_β. Note that for the CNCs prepared in mixed acid medium, a new band appeared at 1730 cm^{-1} corresponding to the existence of carboxyl groups. This indicates that the introduction of nitric acid did cause a significant change in the FT-IR spectra, but the typical structure of the cellulose was preserved (Yu et al. 2013a, b; Zhang et al. 2016; Yu et al. 2016; Hamid et al. 2016). Furthermore, the intensity for the band of carboxyl groups increased first and then decreased with the increase of nitric acids fraction as illustrated in Fig. 4. It is well known that the degree of oxidation could be obtained by calculating the ratio of the intensity of the carbonyl peak to that for the strongest band near 1060 cm^{-1} which is related to the backbone structure of cellulose (Habibi et al. 2006). The calculated DO value listed in Table 2 was 0.05, 0.10, 0.12, 0.11, 0.10 for the ratio of HCl and HNO_3 of 9:1, 8:2, 7:3, 6:4 and 5:5, respectively. It is obvious that the degree of oxidation exhibited a maximum value of 0.12 occurred for the CNCs prepared at the ratio of HCl and HNO_3 of 7:3. This result was consistent with zeta potential measurement. The DO value was also calculated by using the equation: $DO = 0.01 + 0.7(I1735/I1060)$ (Cheng et al. 2014; Mascheroni et al. 2016). The DO values of CCNCs prepared under the ratio of HCl and HNO_3 of 9:1, 8:2, 7:3, 6:4 and 5:5 were 0.04, 0.08, 0.12, 0.11 and 0.08, respectively. In addition, the $–CH_2$ bands around 2900 and 1282 cm^{-1} still appeared in the infrared spectra for the CCNCs (Castro-Guerrero and Gray 2014). It is known that this group is present only at the primary C6 position for untreated cellulose, and

Table 2 The degree of oxidation (DO), crystallinity index (CrI) and thermal parameters for the CNCs and CCNCs prepared under various acidic conditions

Sample	HCl:HNO$_3$ (v/v)	FT-IR DO	CrI (%)[a]	T$_0$ (°C)[b]	T$_{5\%}$ (°C)[b]	T$_{max}$ (°C)[b]
MCCs			83.5			
CNCs	10:0	0	89.4	336.6	322.0	356.5
CCNCs	9:1	0.05	90.1	321.5	274.8	354.3
	8:2	0.10	91.3	321.0	269.5	352.9
	7:3	0.12	91.7	319.3	264.5	349.9
	6:4	0.11	91.5	320.2	265.5	351.5
	5:5	0.10	91.2	320.7	266.7	355.2

[a] CrI was calculated from the XRD patterns

[b] T$_0$ and T$_{max}$ were calculated from the TGA curves

during acid hydrolysis process, the C6 was likely to be preferentially oxidized to carboxylic acid. Therefore it is suggested that the oxidation reaction took place only on the surface of cellulose crystal and amorphous region, whereas the bulk of the nanocrystals were not oxidized.

Conductometric titration

The degree of oxidation (DO) represents the number of primary hydroxyl groups that have been converted to carboxyl groups per anhydroglucose unit after the oxidation process, and the content of carboxyl groups on the CCNCs can be determined by conductometric titration. Figure 5 shows the degree of oxidation for the CCNCs prepared at various nitric acid fractions,
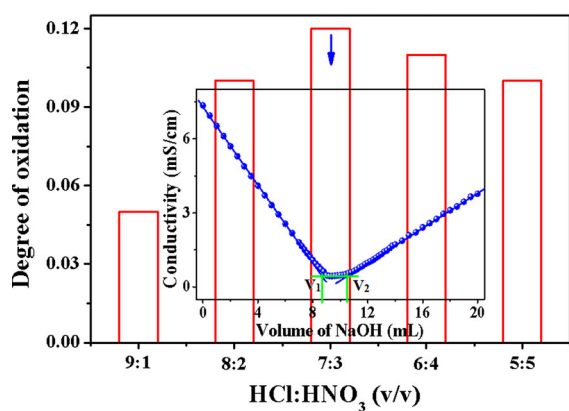

Fig. 5 The degree of oxidation as a function of nitric acid fraction for the CCNCs prepared at various nitric acid fractions. The inset displays a conductometric titration curve of the CCNCs for the ratio of HCl and HNO$_3$ of 7:3

and the inset gives the conductometric titration curve of the CCNCs for the ratio of HCl and HNO$_3$ of 7:3. The carboxyl content of the sample was determined from the conductometric titration curve, assuming that each added molecule of NaOH with this range neutralized exactly one carboxyl group (Mascheroni et al. 2016; Araki et al. 1998). According to the volume of the consumption of NaOH solution, the DO value could be calculated from a conductometric titration curve as illustrated in the inset in Fig. 5. The lowest DO value of CCNCs was obtained when only 10% nitric acid was added into the reaction system. With the increase of nitric acid fraction, the DO value increased first and then decreased. A maximum DO value of 0.123 was achieved for the ratio of HCl and HNO$_3$ of 7:3, being in agreement with that obtained by FT-IR and close to those measured for TEMPO or APS oxidation system (Habibi et al. 2006; Montanari et al. 2005; Castro-Guerrero and Gray 2014; Lam et al. 2012b). Theoretically, the maximum degree of oxidation of CNC is 0.2 (Lam et al. 2012b). According to the DO value obtained from infrared spectra or conductometric titration, it is believed that about 60% of hydroxyl groups could be oxidized to carboxyl groups.

Crystalline structure

Figure 6 illustrates X-ray diffraction (XRD) patterns for the CNCs and CCNCs prepared at various nitric acid fractions, and their crystallinity indexes (CrIs) are summarized in Table 2. All the CNCs exhibited five reflection peaks at 14.6°, 16.6°, 20.5°, 22.6° and 33.8°, corresponding to the typical reflection planes of cellulose Iß (1$\bar{1}$0), (110), (012), (200) and (040),
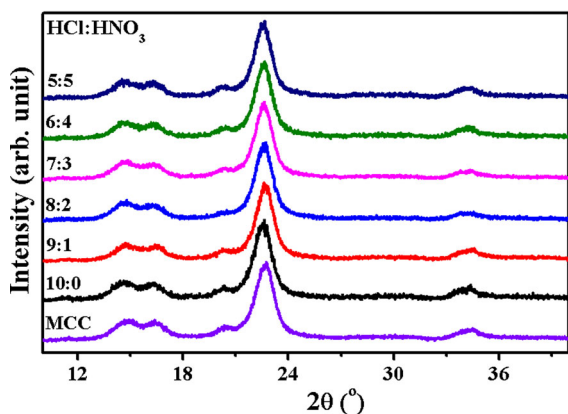
Fig. 6 XRD spectra of CNCs and CCNCs prepared under various acidic conditions

respectively (Yu et al. 2013a, b; Zhang et al. 2016; Cheng et al. 2014; Sun et al. 2016a; Henrique et al. 2015). Note that all of the CNCs gave similar diffraction patterns, implying that their crystal structures did not change during the mixed acid hydrolysis. However, a slight change on the peak width of (200) planes could be observed especially for the ratio of 7:3. Compared with other samples, the peak at 22.6° became broad, indicating a reduction in crystallite dimension. During the hydrolysis process, on the one hand, efficient removal of noncellulosic polysaccharides and dissolution of amorphous zones would take place, being responsibled for the extraction of the CNCs with high crystallinity. On the other hand, partly crystalline region could be destroyed, resulting in smaller crystallite sizes. As shown in Table 2, the CrI increased from 83.5% for the MCCs to 89.4% for the CNCs exacted from the MCCs through pure hydrochloric acid hydrolysis under hydrothermal condition. With the increase of nitric acid fraction, the CrI would further increased in the presence nitric acid, and exhibited a maximum value of 91.7% at the ratio of HCl and HNO_3 of 7:3. In fact, only a slight change in the CrI could be observed, implying nitric acid should play an important role on the oxidation of cellulose but not on the improvement on the crystallinity. That is to say, only the surface of crystalline cellulose was partially carboxylated, and the main crystal structure did not get greatly affected by the oxidative process induced by HNO_3 (Zhang et al. 2016; Cheng et al. 2014; Castro-Guerrero and Gray 2014; Leung et al. 2011).

Possible mechanism

Based on above results, a possible mechanism on the formation of CCNCs has been proposed as shown in Fig. 7. It has been demonstrated that adequately removal of the amorphous region of MCCs can be achieved through hydrochloric acid hydrolysis under high pressure and high temperature reaction condition, but only the surface of crystalline cellulose is attacked by hydrochloric acid (Yu et al. 2013a, b). When nitric acid was introduced into reaction system, the conversion of the cellulose primary hydroxyl groups to carboxyl groups carried out. These oxidation reaction took place firstly on the amorphous region of the MCCs, and then the surface of CNCs. The introduction of carboxyl groups is helpful to promote the degradation of amorphous region, resulting in larger reduction on the acid concentration and particle dimension but remaining almost same crystallinity. However, the increase in the nitric acid fraction corresponded to the reduction in the hydrochloric acid content. With the nitric acid content further increased, the ability for the degradation of cellulose was weakened, resulting in the increase on the yield and particle dimension but decrease on the degree of oxidation of the CCNCs. The maximum degree of oxidation obtained at the volume ratio of HCl/HNO_3 of 7:3 could be mainly contributed to the largest surface area (the smallest size) of CCNC as displayed in Fig. 7.

Thermal stability

Figure 8 shows TGA curves for the CNCs and CCNCs prepared under various reaction conditions, and the thermal parameters are listed in Table 2. Note that all the samples exhibited mainly a one-step degradation process which could be divided into four stages. The removal of water absorbed within cellulose and/or low weight molecules adsorbed on the surface of the nanocrystals occurred first before 120 °C, being responsible for ∼3% of the total weight loss on average of the samples. Then a plateau appeared until about 260 °C, and followed by a sharp decrease in weight at approximately the temperature range from 260–400 °C. Cellulose degradation consisted mainly of several concurrent processes such as depolymerization, dehydration and decomposition of glycosidic units (Yu et al. 2013a, b; Cheng et al. 2014; Henrique
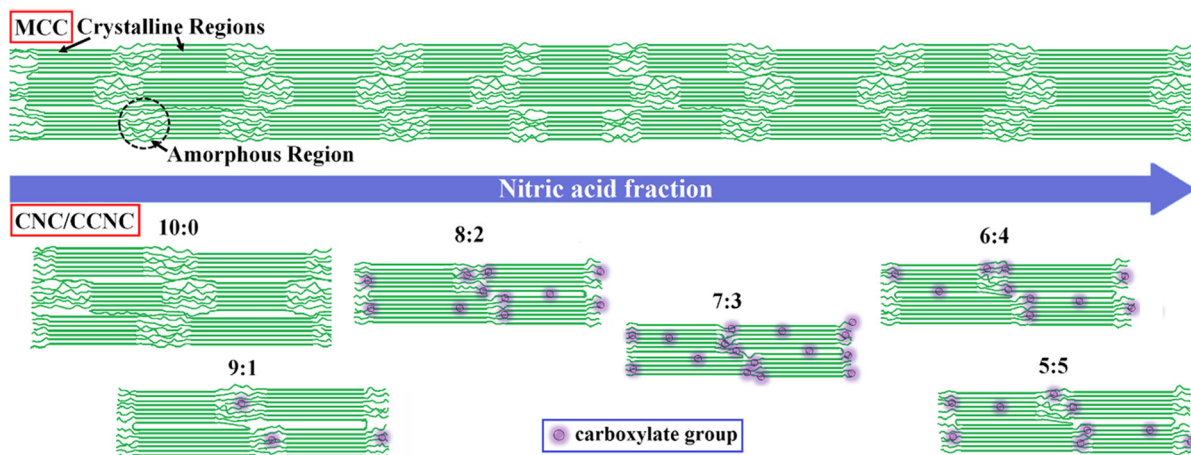
Fig. 7 Possible mechanism on the formation of CCNCs extracted from the MCCs through mixed acid hydrolysis under hydrothermal condition
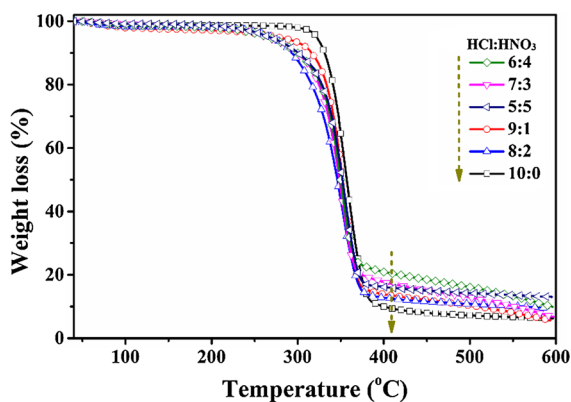

Fig. 8 TGA curves for the CNCs and CCNCs prepared under various acidic conditions

et al. 2015). Final carbonation conversion of the residual products took place over 400 °C. As displayed in Table 2, the T_0, $T_{5 \%}$ and T_{max} of the CNCs prepared through single acid hydrolysis were about 336.6, 322.0 and 356.5 °C, respectively. Compared with the CNCs, all the CCNCs exhibited a slightly decrease in the thermal stability due to the existence of carboxyl groups and small dimension (Zhang et al. 2016; Xiong et al. 2012). Furthermore, the thermal stability of CCNCs firstly became weaken with the increase of nitric acid content in mixed acid medium, and then improved gradually. The CCNCs prepared for the ratio of HCl and HNO$_3$ of 7:3 exhibited the poorest thermal stability, and its T_0, $T_{5\%}$ and T_{max} were about 319.3, 264.5 and 349.9 °C, respectively, being in good agreement with the previous results.

Conclusion

A facile and rapid one-step approach has been presented to prepare CCNCs with high suspension stability and enriched carboxyl groups, which would make these nanoparticles more reactive and extend their potential applications. By using the mixed acid of HCl and HNO$_3$ the conversion of the cellulose primary hydroxyl groups to carboxyl groups can be achieved within short oxidation time without special pre- or post- treatment, acid concentration can also be reduced. The influences of nitric acid fraction on the morphology, microstructure and properties of CCNCs were discussed. The maximum degree of oxidation of 0.12, being close to those through long time oxidation treatment by using TEMPO-mediated and APS as the oxidation reagent. Moreover, smaller dimension, higher crystallinity and relatively high yield of up to 72.6% can be obtained at the ratio of HCl and HNO$_3$ of 7:3. The incorporation of HNO$_3$ into HCl hydrolysis under hydrothermal condition make simultaneous extraction and oxidation of cellulose nanocrystals more efficient and more environmentally friendly.

References

Araki J, Wada M, Kuga S, Okano T (1998) Flow properties of microcrystalline cellulose suspension prepared by acid treatment of native cellulose. Colloid Surf A 142(1):75–82

Bhattacharjee S (2016) DLS and zeta potential—what they are and what they are not? J Control Release 235:337–351

Camarero Espinosa S, Kuhnt T, Foster EJ, Weder C (2013) Isolation of thermally stable cellulose nanocrystals by phosphoric acid hydrolysis. Biomacromol 14(4):1223–1230

Castro-Guerrero CF, Gray DG (2014) Chiral nematic phase formation by aqueous suspensions of cellulose nanocrystals prepared by oxidation with ammonium persulfate. Cellulose 21(4):2567–2577

Chen GY, Yu HY, Zhang CH, Zhou Y, Yao JM (2016a) A universal route for the simultaneous extraction and functionalization of cellulose nanocrystals from industrial and agricultural celluloses. J Nanopart Res 18(2):1–14

Chen L, Zhu JY, Baez C, Kitin P, Elder T (2016b) Highly thermal-stable and functional cellulose nanocrystals and nanofibrils produced using fully recyclable organic acids. Green Chem 18(13):3835–3843

Cheng M, Qin ZY, Liu YN, Qin YF, Li T, Chen L, Zhu MF (2014) Efficient extraction of carboxylated spherical cellulose nanocrystals with narrow distribution through hydrolysis of lyocell fibers by using ammonium persulfate as an oxidant. J Mater Chem A 2(1):251–258

Domingues RM, Gomes ME, Reis RL (2014) The potential of cellulose nanocrystals in tissue engineering strategies. Biomacromol 15(7):2327–2346

Eyley S, Thielemans W (2014) Surface modification of cellulose nanocrystals. Nanoscale 6(14):7764–7779

Fujisawa S, Saito T, Kimura S, Iwata T, Isogai A (2013) Surface engineering of ultrafine cellulose nanofibrils toward polymer nanocomposite materials. Biomacromol 14(5):1541–1546

Habibi Y, Chanzy H, Vignon MR (2006) TEMPO—mediated surface oxidation of cellulose whiskers. Cellulose 13(6):679–687

Hamid SBA, Zain SK, Das R, Centi G (2016) Synergic effect of tungstophosphoric acid and sonication for rapid synthesis of crystalline nanocellulose. Carbohydr Polym 138:349–355

Henrique MA, Neto WPF, Silvério HA, Martins DF, Gurgel LVA, da Silva Barud H, de Morais LG, Pasquini D (2015) Kinetic study of the thermal decomposition of cellulose nanocrystals with different polymorphs, cellulose I and II, extracted from different sources and using different types of acids. Ind Crop Prod 76:128–140

Hosseinidoust Z, Alam MN, Sim G, Tufenkji N, van de Ven TG (2015) Cellulose nanocrystals with tunable surface charge for nanomedicine. Nanoscale 7(40):16647–16657

Jiang F, Esker AR, Roman M (2010) Acid-catalyzed and solvolytic desulfation of H_2SO_4—hydrolyzed cellulose nanocrystals. Langmuir 26(23):17919–17925

Jonoobi M, Oladi R, Davoudpour Y, Oksman K, Dufresne A, Hamzeh Y, Davoodi R (2015) Different preparation methods and properties of nanostructured cellulose from various natural resources and residues: a review. Cellulose 22(2):935–969

Kumar V, Yang T (2002) HNO_3/H_3PO_4–$NaNO_2$ mediated oxidation of cellulose—preparation and characterization of bioabsorbable oxidized celluloses in high yields and with different levels of oxidation. Carbohydr Polym 48(4):403–412

Lam E, Male KB, Chong JH, Leung AC, Luong JH (2012a) Applications of functionalized and nanoparticle—modified nanocrystalline cellulose. Trends Biotechnol 30(5):283–290

Lam E, Leung AC, Liu Y, Majid E, Hrapovic S, Male KB, Luong JH (2012b) Green strategy guided by Raman spectroscopy for the synthesis of ammonium carboxylated nanocrystalline cellulose and the recovery of byproducts. ACS Sustain Chem Eng 1(2):278–283

Leung AC, Hrapovic S, Lam E, Liu Y, Male KB, Mahmoud KA, Luong JH (2011) Characteristics and properties of carboxylated cellulose nanocrystals prepared from a novel one-step procedure. Small 7(3):302–305

Mascheroni E, Rampazzo R, Ortenzi MA, Piva G, Bonetti S, Piergiovanni L (2016) Comparison of cellulose nanocrystals obtained by sulfuric acid hydrolysis and ammonium persulfate, to be used as coating on flexible food-packaging materials. Cellulose 23(1):779–793

Montanari S, Roumani M, Heux L, Vignon MR (2005) Topochemistry of carboxylated cellulose nanocrystals resulting from TEMPO—mediated oxidation. Macromolecules 38(5):1665–1671

Moon RJ, Martini A, Nairn J, Simonsen J, Youngblood J (2011) Cellulose nanomaterials review: structure, properties and nanocomposites. Chem Soc Rev 40(7):3941–3994

Qin ZY, Tong G, Chin YF, Zhou JC (2011) Preparation of ultrasonic-assisted high carboxylate content cellulose nanocrystals by TEMPO oxidation. BioResources 6(2):1136–1146

Sharma PR, Varma AJ (2014) Functionalized celluloses and their nanoparticles: morphology, thermal properties, and solubility studies. Carbohydr Polym 104:135–142

Sirviö JA, Honkaniemi S, Visanko M, Liimatainen H (2015) Composite films of poly (vinyl alcohol) and bifunctional cross-linking cellulose nanocrystals. ACS Appl Mater Int 7(35):19691–19699

Sirviö JA, Visanko M, Liimatainen H (2016) Acidic deep eutectic solvents as hydrolytic media for cellulose nanocrystal production. Biomacromol 17(9):3025–3032

Sun B, Yu HY, Zhou Y, Huang Z, Yao JM (2016a) Single-step extraction of functionalized cellulose nanocrystal and polyvinyl chloride from industrial wallpaper wastes. Ind Crop Prod 89:66–77

Sun B, Zhang M, Hou Q, Liu R, Wu T, Si C (2016b) Further characterization of cellulose nanocrystal (CNC) preparation from sulfuric acid hydrolysis of cotton fibers. Cellulose 23(1):439–450

Xiong R, Zhang X, Tian D, Zhou Z, Lu C (2012) Comparing microcrystalline with spherical nanocrystalline cellulose from waste cotton fabrics. Cellulose 19(4):1189–1198

Xu YH, Liu X, Liu X, Tan JL, Zhu HL (2014) Influence of HNO$_3$/H$_3$PO$_4$–NaNO$_2$ mediated oxidation on the structure and properties of cellulose fibers. Carbohydr Polym 111:955–963

Yang H, Alam MN, van de Ven TG (2013) Highly charged nanocrystalline cellulose and dicarboxylated cellulose from periodate and chlorite oxidized cellulose fibers. Cellulose 20(4):1865–1875

Yu HY, Qin ZY, Liang BL, Liu N, Zhou Z, Chen L (2013a) Facile extraction of thermally stable cellulose nanocrystals with a high yield of 93% through hydrochloric acid hydrolysis under hydrothermal conditions. J Mater Chem A 1(12):3938–3944

Yu XL, Tong S, Ge M, Wu L, Zuo J, Cao C, Song W (2013b) Adsorption of heavy metal ions from aqueous solution by carboxylated cellulose nanocrystals. J Environ Sci 25(5):933–943

Yu HY, Zhang DZ, Lu FF, Yao J (2016) New approach for single − step extraction of carboxylated cellulose nanocrystals for their use as adsorbents and flocculants. ACS Sustain Chem Eng 4(5):2632–2643

Zhang K, Sun P, Liu H, Shang S, Song J, Wang D (2016) Extraction and comparison of carboxylated cellulose nanocrystals from bleached sugarcane bagasse pulp using two different oxidation methods. Carbohydr Polym 138:237–243